Received: 17 October 2019 | Revised: 7 March 2020 | Accepted: 19 March 2020

DOI: 10.1002/jbm.b.34614

ORIGINAL RESEARCH REPORT

Society For Biomaterials | WILEY

Novel lactone-layered double hydroxide ionomer powders for bone tissue repair

Tianhao Zhou[1] | Edward D. McCarthy[2] | Constantinos Soutis[1] | Sarah H. Cartmell[1]

[1]School of Materials, The University of Manchester, Manchester, UK

[2]School of Engineering, The University of Edinburgh, Edinburgh, UK

Correspondence
Sarah H. Cartmell, School of Materials, The University of Manchester, Oxford Road, Manchester, M13 9AX, UK.
Email: sarah.cartmell@manchester.ac.uk

Funding information
Engineering and Physical Sciences Research Council, Grant/Award Number: EP/I02249X/1

Abstract

This article describes the use of a novel lactone-layered double hydroxide polymer network (PN), derived from a poly(lactide-co-caprolactone) copolymer, as a controlled ion-release agent for artificial bone tissue regeneration. The osteogenic cell culture Saos-2 is used as a test culture to investigate the PN's performance as an extracellular ion-release agent. The compelling performance of this PN is demonstrated in both growth and osteogenic media compared with a control of cells grown on tissue culture plastic (TCP) without PN. Firstly, the PNs released concentration of magnesium ions over time ranging from 10 to 60 mM after 24 hr, depending on the PN sample. After incubation of Saos-2 with the PN, while no difference was seen in cell number, there was significant upregulation of bone-related gene expression at 14 days—~5fold increase in Bone Morphogenetic Protein 2, ~3fold increase in osteopontin and ~2fold increase in collagen Type I. In addition, normalized alkaline phosphatase activity was seen to significantly increase by ~2fold with PN presence. A ~4fold increase in collagen Type I protein expression (via Gomori Trichrome Stain) was observed with PN presence. In addition, a ~4fold increase in phosphate deposits (as seen with Von Kossa staining analysis) was seen with PN presence. It is found that this novel PN material has a significant potential for bone tissue regeneration.

KEYWORDS

bone repair, layered double hydroxide, polycaprolactone, polylactic acid, SAOS2

1 | INTRODUCTION

Bone defects are common occurrences in the population and can result from incidences such as traumatic injury. Clinically, these defects can be repaired by the use of various types of grafts; however, due to limited natural tissue availability and expense, alternative measures in clinical practice need to be developed. Bone tissue engineering approaches (e.g., the use of bioactive bone graft substitutes) are demonstrating increasing potential for use as alternative therapies for bone defects and deformities (Feng & McDonald, 2011).

A bone tissue matrix consists of two components, an organic and inorganic phase. The organic phase is approximately 20 wt% of the bone and comprises mostly collagen (around 90 wt% Type I collagen). The collagen macromolecule has a specific structure of three polypeptide chains wound into a repeating triple-helix fibril (Ramachandran, Venkatachalam, & Krimm, 1966). The inorganic matrix mainly consists of apatite crystals. Many different elements are present in this component, for instance, calcium, phosphorous, sodium, and magnesium. All these ions are present in the crystal apatite (mainly in the form of calcium hydroxyapatite $Ca_{10}PO_4OH_2$, HA) that is formed in the bone cell matrix, and which provides the stiffness of the tissue, while collagen provides the bone with flexibility.

Osteoblasts, which secrete bone proteins and minerals, are responsible for the production of the cell matrix. They also control the flux of

ions in the extracellular cycle. The collagenous extracellular matrix (ECM) an osteoblast produces has an important effect on cell activity; for example, it can act as a nucleation site for mineralization. Specifically, collagen Type I fibrils function as a template for mineral deposition and provide the initiation sites for mineral crystallization. Furthermore, osteoclasts are responsible for bone tissue resorption (Bullough, 2010) and with the correct compositional balance of osteoblasts and osteoclasts, bone remodeling can be well regulated. A compositional imbalance of these two cell types results in osteoporosis, (Feng & McDonald, 2011).

One approach to enhance bone cell activity is the addition of inorganic ions. For example, it has been well documented that Ca^{2+} can stimulate bone cell proliferation and differentiation (Zhou et al., 2010). Meanwhile, research has also shown enhanced new bone formation both in vitro and in vivo using Mg^{2+} (Yamasaki et al., 2002; Yamasaki et al., 2003; Zreiqat et al., 2002). The incorporation of inorganic ions is controllable, and it is a cost-efficient approach compared with current stimulatory approaches such as injection of growth factors (e.g., bone morphogenetic protein 2, an essential protein for the development of bone and cartilage) directly to the bone defect site. Multiple inorganic ions have been studied for this specific purpose, and also for osteogenesis, angiogenesis (Gorustovich, Roether, & Boccaccini, 2010), and antibacterial activity (Jones, Ehrenfried, Saravanapavan, & Hench, 2006). However, most of the cases have used bioactive glass (Si-based), which was first identified and synthesised by L Hench et al. (Hench, Splinter, Allen, & Greenlee, 1971). Bioactive glasses have been actively used for bone-related applications (Gough, Jones, & Hench, 2004). Polymers, by contrast, have been less well studied as potential ion release media by themselves. However, polymer properties are easily tuned (i.e., their mechanical properties, chemical properties, and degradation properties) according to the particular requirements of an application in a way that glass matrices cannot. For instance, the manipulation of the monomer types and ratios in a polymer can result in lower stiffness in the polymer materials in contrast to bioglass. Such changes in the matrix modulus can positively affect the differentiation of cells. Park et al. stated that a modulus of 1 kPa can lead to chondrogenic differentiation (Park et al., 2011), while for bone differentiation, Lu et al. recommended an optimal stiffness range of higher than 25–40 kPa (Lv et al., 2015).

The aim of this work is to study the effect of the insoluble lactone (LC INSOL) polymer network derived from a lactide-caprolactone copolymer on stimulating osteogenesis in vitro. The LC INSOL is incubated indirectly with the osteoblast-like cell type, Saos-2. The effects of extracellular ions eluted from LC INSOL on the cell matrix, specifically on the formation of the organic and inorganic components, are investigated. The study is focused on the ion release of the Mg^{2+}-eluting LC INSOL and on the influence of the ions released from this PN on human osteosarcoma cells. The cytotoxicity of the Mg^{2+} and Al^{3+}-ion eluting PN is investigated via indirect in vitro tests, and its effect on differentiation and mineralization of the osteoblast-like cells in vitro is determined.

2 | MATERIALS AND METHODS

The ε-caprolactone (97%) was obtained from Aldrich and stored at 4°C before use, while the L,D-lactide (99%) was supplied by Alfa Aesar. Both materials were used as monomers in the polymerization process. The initiator, synthetic-layered double hydroxide carbonate (LDH-carbonate), was obtained from Aldrich. LDH-carbonate has a layered structure with a high anionic exchange capacity that allows it to host and release various anionic compounds. Its chemical formula is $Mg_6Al_2(CO_3).(OH)_{16}.4H_2O$. Since L,D-lactide, ε-caprolactone and LDH-carbonate are all sensitive to moisture, it is essential to avoid their re-adsorption of water; hence, they were both stored in a desiccant. L,D-lactide was sublimed immediately prior to reaction to remove moisture.

3 | SAMPLE PREPARATION

The lactone PN LC INSOL was selected from nine other PNs synthesized in a previous study (Zhou, McCarthy, Soutis, & Cartmell, 2018) as the optimal one for use in osteogenesis due to its high polymer mass yield and high magnesium content; a schematic of the LC INSOL preparation process is given in Figure 1 (Zhou et al., 2018). This comprised the polymerization of a mixture of monomer(s) plus LDH followed by dissolution of the product in methylene chloride. The solution was then centrifuged to result in an insoluble residue, which was dried to result in two separate phases of the polymer, soluble (SOL) and insoluble (INSOL). The latter was the PN used in this study, which was then ground prior to use.

4 | CHARACTERISATION METHODS

4.1 | pH-time measurements of polymer networks in various media

To better understand the pH time response of the LC INSOL, it was rinsed in an aqueous environment, 100 mg of LC INSOL fragments were rinsed in 2 mL of DI-water (two repeats) at 37°C in 15 mL centrifuge tubes (similar sample surface areas). pH measurements were repeated at various time

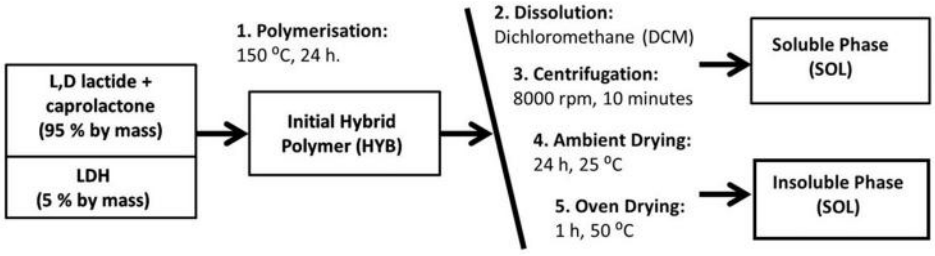

FIGURE 1 Schematic of PN preparation process (Zhou et al., 2018)

points (at 6 hr, every single day in the first week, at 2 weeks and at 3 weeks). Two sets of experiments were performed, with and without 10% NaOH neutralization to pH 7 after each time measurement, to best mimic the buffering effect existing in the culture medium.

4.2 | Inductively-coupled plasma optical emission spectroscopy (ICP-AES)

The ionic concentrations of released magnesium (Mg^{2+}) and aluminium (Al^{3+}) ions of LC INSOL were determined using ICP-AES (Optima 5300DV manufactured by Perkin-Elmer). This was performed after immersion of ground PN powder in phosphate buffered saline (PBS) for 24 hr and then in culture medium (McCoy 5a from Sigma) without other additions for different time durations at 37°C in static conditions to mimic cell culture conditions and ion concentrations. Three parallel samples were processed and their supernatants were collected simultaneously. The supernatant samples were diluted in the ratio 1:10 in a 2% HNO_3 matrix before analysis. Three repeats were performed per sample. The measurement wavelengths for the selected elements were 285.213 nm (Mg^{2+}) and 396.153 nm (Al^{3+}), respectively.

4.3 | Cell culture

Osteosarcoma Saos-2 cells were cultured in McCoy 5a with 10% fetal bovine serum (FBS), 1% L-Glucose, and 1% antibiotics (penicillin/streptomycin) as the general growth medium (GM). Osteogenic medium (OM) was also prepared, which contained all components in GM as well as 50 μg/mL Ascorbate-2-phosphate (Ascorbic acid), 10 mM β-glycero phosphate (β-Gly), and 10 nM dexamethasone (Dex). A 75 mL tissue culture flask with 100,000 cells was incubated at 37°C in a humidified incubator with 5% CO_2. The medium was changed twice a week, and cells were subcultured when they reached 75% confluency.

Thirty thousand cells were placed into every well of a 12-well plate (8,000 cells/cm^2) for cell seeding. Bio-inserts from Greiner Bio One with 1 μm pore size were used to hold the LC INSOL powder samples in the wells at 3.125, 6.25, 12.5, and 25 mg/mL mass concentrations to culture medium, respectively, as shown in the schematic, Figure 2. Four biological replicates were performed for each sample for all the following experiments. Figure 3 is a schematic of the assays performed on the specimens over 14 days.

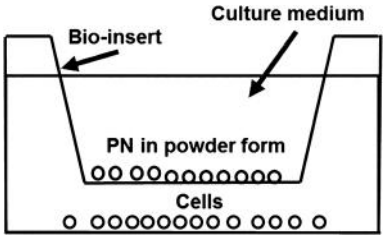

FIGURE 2 Schematic of Saos-2 osteosarcoma cell line indirectly cultured with PNs in bio-inserts with various mass concentrations using 12-well plate

4.4 | Pico green assay for DNA quantification

When the cells were cultured for 7 days and 14 days, respectively, they were then washed twice with PBS in the well plate, and three freeze–thaw cycles were performed using 700 μL Tris buffer (100 mM) per sample at a temperature of −80°C. Quant-iT PicoGreen dsDNA Assay Kit from Thermo Fisher Scientific was used for the assay. Hundred microliter cell lysate from the freeze–thaw cycle and 100 μL Pico Green reagent were mixed and covered in foil from light for 30 min at room temperature based on the protocol provided in the kit. After this, the fluorescence of the sample mixture was measured in a 12-well plate at excitation and emission wavelengths of 485 and 535 nm, respectively, using a Fluostar Optima plate reader, (BMG Labtech). The final DNA concentration was calculated using a standard curve provided in the kit that was obtained from a pure double-strand DNA. This assay was applied to the Saos-2 cultured at different conditions as described later on.

4.5 | Alkaline phosphatase activity (ALP)

Aliquots from the same solution used in the Pico Green assay were mixed with the p-nitrophenyl phosphate (pNPP) working solution as the phosphate substrate, which turns yellow when dephosphorylated

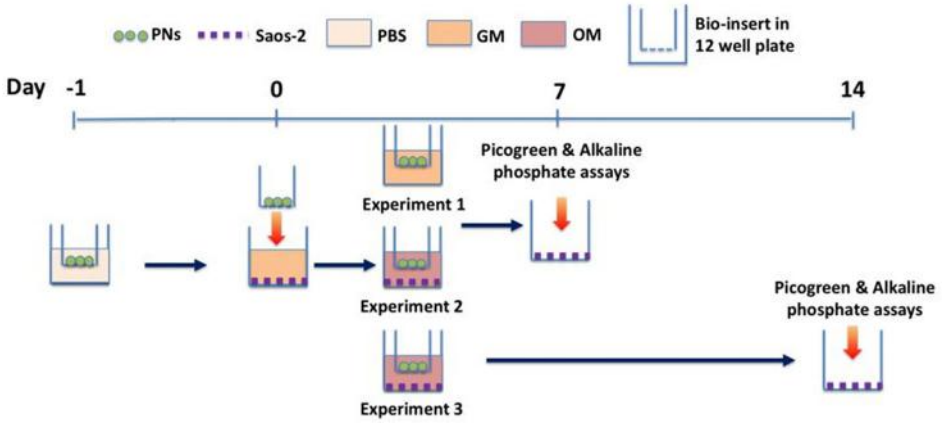

FIGURE 3 Schematic of Saos-2 osteosarcoma cell line indirectly cultured with PNs in bio-inserts with various mass concentrations using a 12-well plate for Picogreen and alkaline phosphate (ALP) assays at Day 7 and 14, respectively (LC INSOL applied in both growth media (GM) and osteogenic media (OM) for 7 days and 14 days). PNs, polymer networks; PBS, phosphate buffered saline; GM, growth media; OM, osteogenic media

by ALP (purchased from Biovision). The standard curve was prepared according to the manufacturer's instructions and was used to calculate the absolute ALP activity. The reaction lasted for 60 min and was covered from light at room temperature. Absorbance was measured at 405 nm wavelength using a spectrometer from Labsystems, Multiskan Ascent. The ALP activity was calculated by Equation (1), where A represents the pNP generated by the samples in nmol, V is the sample volume added in each well in milliliters.

$$\text{ALP activity} = A/V \quad (1)$$

4.6 | Gomori trichrome for collagen histology staining

In order to make Gomori solution, 0.6 g of chromotrope 2R (TCS bioscience ltd), 0.3 g of fast green FCF (Fisher), and 0.6 g of phosphotungstic acid were mixed with 100 mL of distilled water, while 1 mL of glacial acetic acid was added afterward to acidify the solution. For the cell section, cell monolayers in the well plate were initially rinsed in water and stained with Mayer's haematoxylin for 5 min. Scotts tap water (a blueing reagent designed for histology and cytology) was then used to rinse the cells section for 30 sec. The Gomori solution prepared above was applied for 5 min staining and later on rinsed out with 0.2% acetic acid and distilled water, respectively. Staining colors were blue or grey (nuclei), green (collagen) and red (muscle, cytoplasm, red blood cells and fibrin). The percentage areas of the bone nodules in each well were quantified using ImageJ (1.48v, Wayne Rasband, National Institutes of Health). Specifically, five certain areas (at positions 12, 3, 6, 9 o'clock and center) from each well were selected (×10 magnification were used).

4.7 | Von Kossa histology staining

For the staining process, 5% aqueous silver nitrate, 5% sodium thiosulphate (both obtained from VMR), and 1% neutral red (TCS Bioscience ltd) were prepared in advance. The cells were initially washed by deionized water and covered with filtered 5% aqueous silver nitrate. Then, all the cells in the well plate were moved under UV light with foil put underneath to achieve better lighting conditions because of foil reflecting. A triple de-ionized water wash was performed, and 5% sodium thiosulphate solution was added to the cell matrix for 5 min for the removal of excess silver salt. Next, a 1% neutral red solution was applied as a counterstain. The areas of precipitates were quantified using ImageJ.

4.8 | RNA isolation and cDNA synthesis

The total RNA was extracted from the cell population using a RNeasy mini kit (Qiagen) following the product manual. Before the RNA extraction steps, cells were washed with PBS. Trypsin and centrifuge (300 g, 5 min) were then used to obtain a cell pellet at the bottoms of the centrifuge tubes. Three hundred fifty microliters of RLT buffer (with 1% v/v b-Mercaptoethanol from Sigma) were put into the cell pellet for RNA lysate homogenization using 20G needles to break up the cell membranes. The total volumes of the RNA lysate were made up to 700 μL per sample with 70% ethanol. Then the mixture was then applied to a RNeasy spin column (a silica-gel membrane) and washed twice based on instruction in the protocol. Total RNA was eluted with RNase free water (30 μL as final RNA mixture volume). Subsequently, RNA integrity and concentrations were measured using Nanodrop Lite spectrometer (thermos scientific).

cDNA was used as the template for RT-PCR. A total of 100 ng/mL RNA was used for the reversed transcription and this was performed using QuantiTect, a reversed transcription kit (Qiagen). Specifically, the gDNA were firstly eliminated from the RNA solution using the gDNA wipeout buffer at 42°C for 2 min. The mixture solution was prepared with quantiscript reserve transcriptase, quantiscript RT buffer, and 5X RT primer mixes according to the volume recommended by the kit (1 + 4 + 1 μL, respectively, plus 14 μL genomic DNA) and incubated for 15 min at 42°C and 3 min at 95°C. All the incubation was performed using a Peltier Thermal Cycler (Bio-Rad). After the incubation, the final cDNA solution was stored at −20°C for further experiments.

4.9 | Primers and real-time PCR

To determine whether magnesium has an influence on bone metabolism, several genes that are involved in bone and matrix formation were analyzed. The gene markers were purchased from Quantitect Primer. The primer sequences used were glyceraldehyde 3-phosphate dehydrogenase (GapDH), Bone morphology protein (BMP2; Hs_GAPDH_1_SG QuantiTect Primer Assay/ NM_002046), osteopontin (OPN; Hs_BMP2_1_SG QuantiTect Primer Assay/ NM_001200), osteoclactin (OCN; Hs_BGLAP_1_SG QuantiTect Primer Assay/ NM_199173), and collagen Type I (COL; Hs_COL1A1_1_SG QuantiTect Primer Assay/ NM_000088).

Real-time quantitative PCR (polymerase chain reaction) was used to quantify the expression rate of the selected genes by amplifying the gene signal using thermal cycles. A SYBR Green PCR kit was used (Quantifast from Qiagen). The mixture was mixed using 2X Quantifast SYBR Green PCR master Mix, 10X QuantiTect Primer Assay, Template cDNA and RNase-free water (reagents in the kit). Twenty five microliters of this final mixture were placed into each well in the 96-well plate (life technologies) and sealed with plastic film on the top. Then, a PCR thermal cycler from Applied Biosystems (Thermal Fisher) was used for the qPCR thermal cycles in 2 steps. Specifically, the first step, PCR initial activation step, was performed for 5 min at 95°C. The second cycling step, started with denaturation for 10 s at 95°C, followed by annealing for 30 s at 60°C; 40 cycles were performed for each sample.

The solution was homogenized using a micro centrifuge (Prism Mini). The final gene expression data were chosen to use fold exchange calculated from the original Ct (cycle threshold: the number

of cycles required for the fluorescent signal to cross the threshold [i.e., to exceed background level]). Values were obtained from StepOnePlus software v2.3 (Thermo Fisher Scientific). Gene expression is calculated as normalized fold change compared with that of the house-keeping gene GapDH. The method is detailed further in the literature (Livak & Schmittgen, 2001).

For each assay, $n = 4$ replicates were performed, and data on all graphs are represented as mean values with standard deviation as error bars. Statistical significance was determined using a one-way Analysis of Variance (ANOVA). Significance was defined for p values less than 0.05 and is reported in the figures with an asterisk * (*$p \le .05$, ** $p \le .01$, ***$p \le .005$, ****$p \le .001$).

5 | RESULTS

5.1 | pH measurements

LC INSOL, a lactone copolymer network (PN) with fewer carboxylic units per monomer than poly(lactic acid) was synthesized according to the method described in Zhou et al. (2018). This copolymer PN was subjected to immersion in the culture medium described above. The pH fluctuations of LC INSOL during immersion are presented in Figure 4 at different time intervals up to 3 weeks.

The pH values for LC INSOL in culture medium is lower than that in the medium control due to the high pH value of the original culture medium base (pH = 8.0–8.5). Moreover, due to the buffer system (sodium bicarbonate) in the medium, the pH trend in the latter is better controlled compared to that of the LC INSOL especially before Day 3, which is the first medium replacement point. The clearest trend is that the LC INSOL shows (a) initially more acidic character (lower pH) up to Day 3 and (b) good pH stability from approximately 12 days onwards.

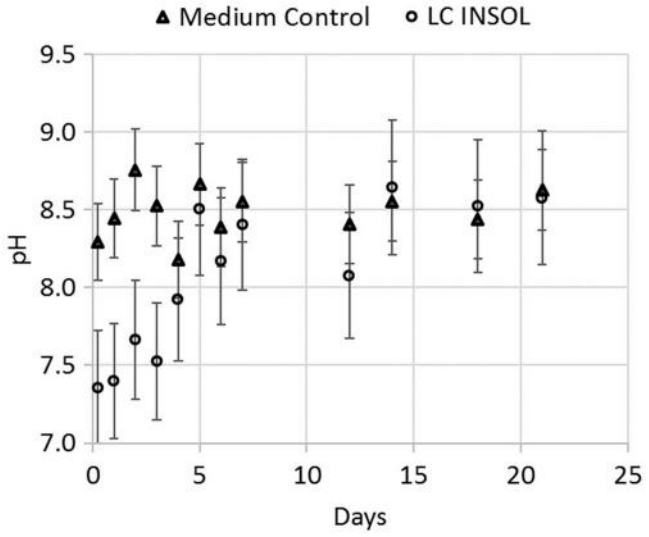

FIGURE 4 pH measurements of LC INSOL with different compositions in completed culture medium up to 3 weeks (mean ± SD [5%], $n = 3$)

5.2 | ICP-AES

After LC INSOL was exposed in PBS for 1 day, the Mg^{2+} ion concentration (Figures 5a,b) measured in the LC INSOL supernatant was approximately proportional to the original mass of Mg^{2+} in the corresponding LDH initiator pre-cursor. The Mg^{2+} concentrations of the LC INSOL supernatant ranged from 9 to 59 mM in the concentration range 3.125–25 mg/mL. In Figure 5a, at 24 hr, the progressive increase of Mg^{2+} concentration from 9.1 mM at 3.125 mg/mL to 58.2 mM at 25 mg/mL is shown. This represents a 6.4-fold increase in Mg^{2+} concentration for an 8-fold increase in LC INSOL concentration. Notionally, this is an Mg^{2+} release efficiency of 80%. In Figure 5b, the progressive reduction of Mg^{2+} concentration from 6.3 to 0.3 Mm between Days 4 and 14 at LC INSOL concentration of 25 mg/mL is shown as a consequence of PBS changes at each time point. Because of the 24 hr peak in Mg^{2+} concentrations, future samples were allowed a 24 hr PBS incubation period prior to cell exposure to ensure the release profile as seen in Figure 5b.

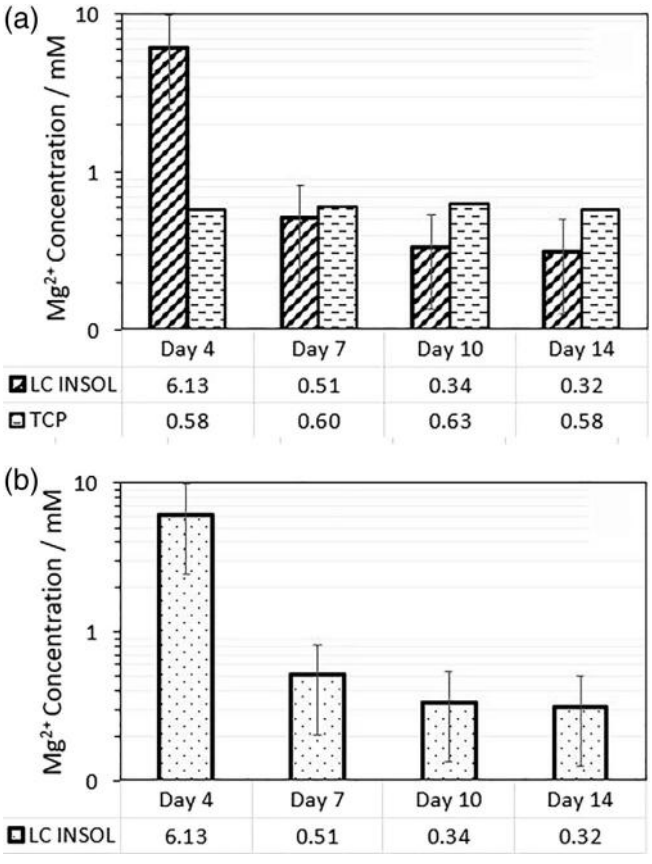

FIGURE 5 (a) ICP-AES measurement of Mg^{2+} ion concentrations after LC INSOL was exposed to PBS at different concentrations for 24 h (Error bars: 5% standard deviation). (b) ICP-AES measurement of Mg^{2+} ion concentration after LC INSOL was exposed to culture medium (basal McCoy 5A [without FBS]) at a concentration of 25 mg/mL at 37 °C (with no cells) at Days 4, 7, 10, and 14. The Mg^{2+} ion concentration for the TCP control medium at each day is also plotted

5.3 | Pico green and ALP assay of saos-2 osteosarcoma cell cultured with bio-inserts

Pico green was used for measuring the DNA concentration of the cells with and without osteogenic induction factors. Generally, LC INSOL had no cytotoxic effects on the cells' degree of proliferation. In Figures 6a,b, the DNA concentration of samples at four concentrations of LC INSOL solution are compared with that for TCP at both 7 and 14 days, respectively, showing no statistically significant difference in DNA concentration at 7 days, but showing a statistically higher DNA concentration at 14 days for a LC INSOL concentration of 6.25 mg/mL.

5.4 | Real-time PCR

Real-time PCR is a technique for detection, determination and comparison of selected genes with a house-keeping gene GapDH, the most common used reference gene. Four bone-related genes were assessed for expression in normalized fold-change (NFC) normalized to TCP controls at Day 14 (Figure 7). Here, both BMP2 and OPN exhibited upregulation at 3.125 mg/mL and 6.25 mg/mL and showed maxima at 12.5 mg/mL (1.56 and 4.73 for BMP2 and OPN) compared with TCP controls, and then decreased considerably at 25 mg/mL (BMP2 = 0.78).

However, for LC INSOL at 25 mg/mL at Day 14, COL NFC almost doubled in value, and it was also significantly higher than the TCP NFC and those of the LC INSOL at other mass concentrations. OCN also showed a significant increase in gene expression on Day 14 at 25 mg/mL mass concentration (fold change of 2.65) compared to that of the TCP. Collagen Type I (COL) also indicated higher NFC compared with that of the TCP (NFC = 4.4). Osteocalcin was the last gene marker to express with a significant upregulated effect for the LC INSOL at 25 mg/mL at day 14 (NFC = 2.6).

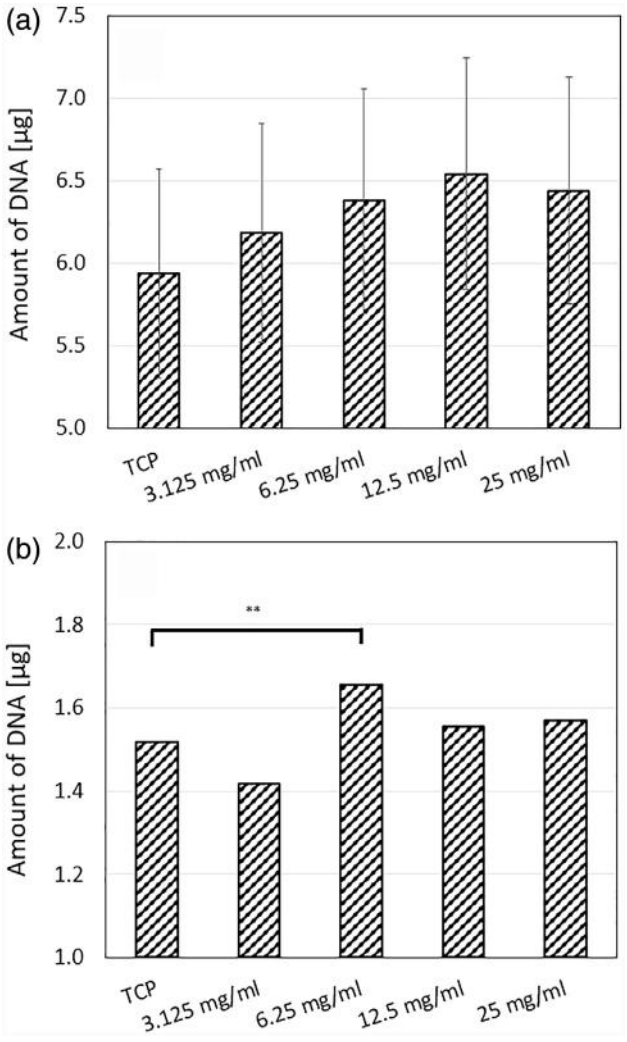

FIGURE 6 DNA amount (Pico Green assay) of cells incubated indirectly in TCP and LC INSOL in osteogenic media at mass concentrations in the range 3.125–25 mg/mL after (a) 7 and (b) 14 days

5.5 | ALP results

In Figure 8, the ALP activity of LC INSOL in osteogenic medium sample group are statistically higher than that of TCP at concentrations higher than 6.25 mg/mL. This is despite the fact that the equivalent dataset for LC INSOL DNA concentrations were not significantly different to that of TCP.

5.6 | Gomori trichrome collagen histology staining

Gomori trichrome is a technique for staining collagen in histology. The collagen generally stains in a blue color, while nuclei, cytoplasma or fibrin stains in red. The responses of the three groups, cultured for different time periods (Days 7, 14, and 21), were studied and recorded.

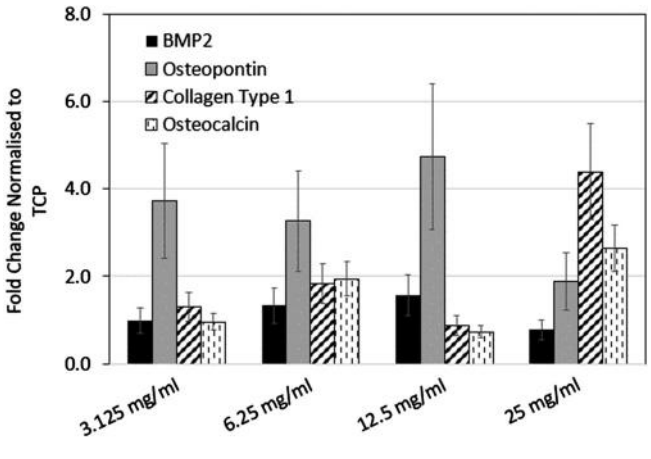

FIGURE 7 Gene expression of 4 gene markers using Saos-2 in OM at 14 days at four different mass concentrations of the samples indirectly exposed and incubated (N = 3) (no significant differences were found in gene expression at Day 7 between mass concentrations)

At both Days 7 and 14 (Figure 9a; A and B), the blue color indicative of collagen increased in intensity with increasing solution concentration from 3.125 to 12.5 mg/mL. The sporadic dark areas in the cell matrix can be attributed to mineralized bone nodules consisting of condensed bone cells (Gough et al., 2004). Inspecting the quantitative data for percent bone nodule area in Figure 9b, it can be seen that mineralization was maximal for the 6.25 mg/mL sample, but it was lower at PN concentrations both below and above this value. This trend was observed at all the three time-points. Samples with LC INSOL concentrations from 3.125 to 12.5 mg/mL indicated a statistically significant increase in nodule area percentage at Day 7 compared with that of the TCP, which was also consistent with the amount of collagen detected as green-stained regions. Nodule areas increased even further by Days 14 and 21. At Day 14, LC INSOL indicated statistical differences in nodule area percentage compared with that of the TCP (Figure 9b). At an LC INSOL concentration of 6.25 mg/mL, the largest number of nodules was observed at both Day 14 and Day 21, and this indicated a significant difference in percent nodule area compared with that of TCP and also those of PNs at different concentrations. However, percent nodule areas were lower in the 12.5 and 25 mg/mL specimens at Day 21.

5.7 | Von Kossa phosphate histology staining

Visualization of the phosphate staining was performed on Day 21 (Figure 10a). In these images, the high phosphate levels are represented by a black dye. The quantification of Von Kossa staining on Day 21 (Figure 10b) was also performed using ImageJ to calculating the percentage area of the phosphate group stains. For the PN solutions, for the three concentrations from 6.25 to 25 mg/mL, the phosphate area percentages were 25.3%, 30.5%, and 37.5% of total specimen area, respectively). By contrast, at 3.125 mg/mL, the phosphate area detected was practically equivalent to that of the TCP control (ca. 5%). Thus, there was significant enhancement of phosphate group production in the PN specimens at concentrations at and above 6.25 mg/mL compared with the TCP control.

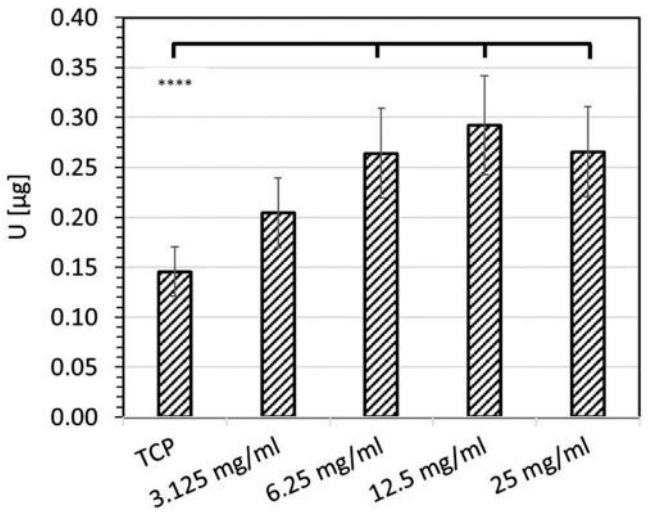

FIGURE 8 ALP activity after 14 days' cell culturing in osteogenic media indirectly exposed to LC INSOL incubated at mass concentrations from 3.125 to 25 mg/mL

6 | DISCUSSION

Due to the nature of the manufacture of the LC INSOL polymer network, it is unable to be employed as a load bearing scaffold. However, it is possible to utilize LC INSOL as either part of a degradable composite or as an ion-release matrix in the form of a powder that could be easily administered to surgical fracture sites. At present, there are only two main types of powders used in surgery for bone repair that are used in this manner. One is vancomycin powder, but this powder mainly functions as an antibiotic for surgical sites rather than as an enhancer for bone formation (Bakhsheshian, Dahdaleh, Lam, Savage, & Smith, 2015). The other 'powder' is BoneGlass (manufactured by Noraker, which fundamentally is bioglass [BG] 45S5). As mentioned previously, for materials such as 45S5 BG, it is difficult to form a 3D structure, which usually has to be manufactured by heating and sintering. Moreover, the desired crystallization is also hard to promote during sintering (Rahaman et al., 2011). Additionally, BG has low strength, which can be disadvantageous for application (Chen, Thompson, & Boccaccini, 2006). Lastly, BGs' relatively slow degradation rate (maximum 60% mass loss over 10 days) can be a serious disadvantage in medical applications, because their degradation rates cannot match that required for optimal tissue growth conditions (Huang, Day, Kittiratanapiboon, & Rahaman, 2006; Huang, Rahaman, Day, & Li, 2006). By contrast, the lactone insoluble polymer network LC INSOL shows faster degradation, which is more suitable (60% mass loss in 7 days). For this reason, LC INSOL was placed in bio-inserts to culture with cells indirectly in vitro. Generally, in the first 4 days, pH values were low; however, as shown in Figure 4, the pH stabilized within a safe range (ca. pH = 8.5) for PN samples in culture medium up to 3 weeks.

ICP-AES measurements were firstly conducted in the basal culture medium without either FBS or cells. This tested the ion release rate from the LC INSOL without the effect of other factors. FBS, as an essential supplement in cell culture, can release amino acids that may affect pH and ion levels due to amino acids' degradation. In Figure 5a, the Mg^{2+} ion concentrations after LC INSOL hydrolysis at 24 hr is presented for LC INSOL mass concentrations in the range 3–25 mg/mL (Mg^{2+} concentrations ranged from 9 to 58 mM for the three different mass concentrations). Any pH change in the solutions was probably neutralized by the PBS buffer itself. Therefore, the rate of degradation of LC INSOL did not appear to have been significantly accelerated by acid release during degradation. In the first 24 hr, when LC INSOL was exposed to PBS, it showed a slightly higher Mg^{2+} concentration. This might have been due to the fact that LC INSOL had lower density and high surface ion transfer area (less spatial restriction). In Figure 5a,b, LC INSOL exhibited excellent ion-eluting ability at Day 4; this was likely due to fast degradation of the copolymer

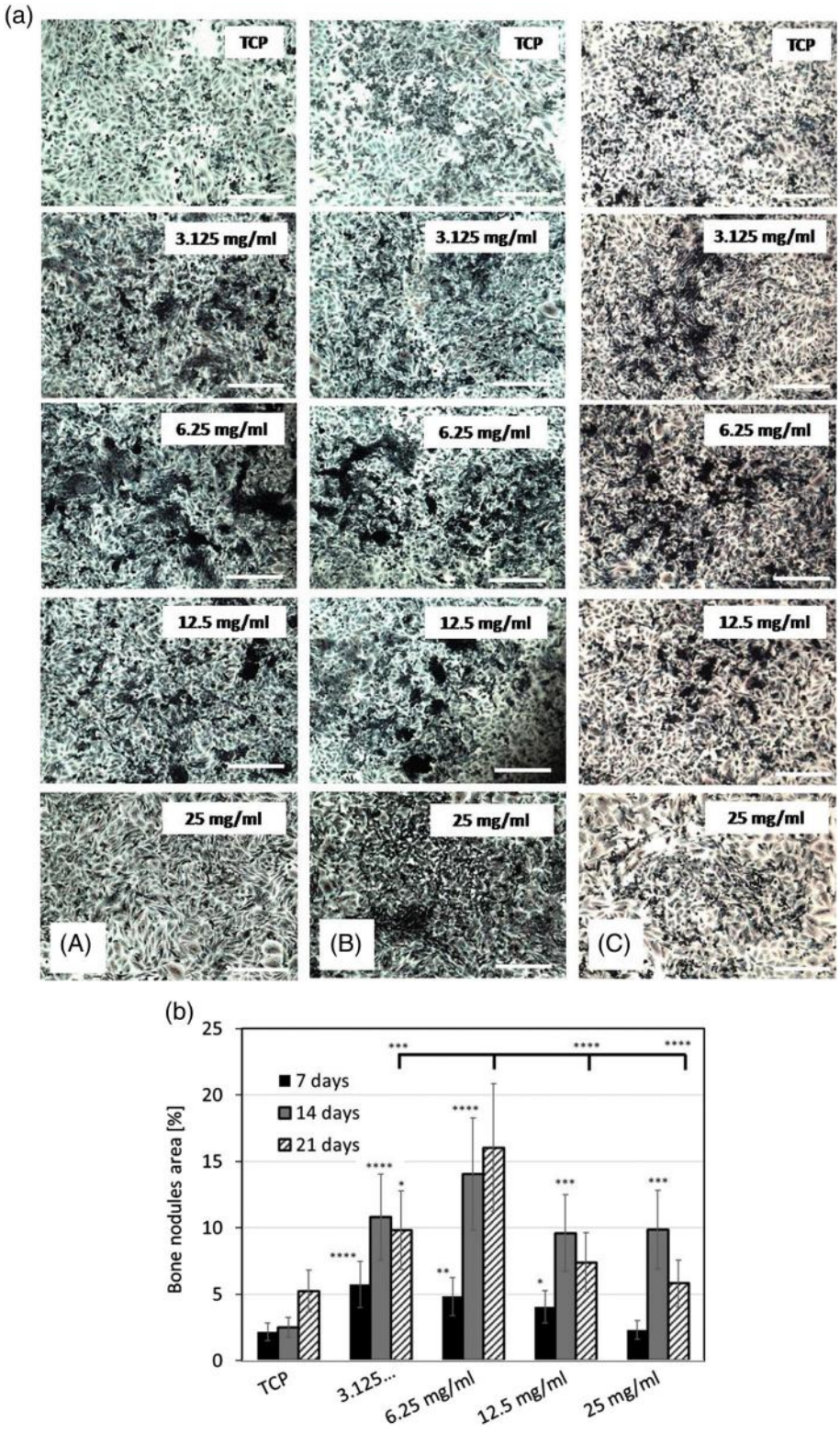

FIGURE 9 (a) Collagen staining of extracellular matrix using Gomori trichrome at (A) Day 7, (B) Day 14, and (C) Day 21 in OM with ×10 magnification (Scale bar = 250 μm). Note that the blue color indicative of collagen increased in intensity with increasing solution concentration from 3.125 to 12.5 mg/mL. (b) Quantification of nodule percentage-of-area from Gomori trichrome staining in each well at (A) Day 7, (B) Day 14, and (C) Day 21 in OM with ×10 magnification (statistical analysis was performed on the nodule area [%] of LC INSOL at various mass concentrations and TCP at the same time point as well as that in LC INSOL at 6.25 mg/mL with the other mass concentrations)

backbone, (Lyu & Untereker, 2009), indicated by the accompanying pH drop to Day 4 (Figure 4).

Three osteosarcoma cell lines MG63, Saos-2, and U2OS are frequently used for comparative study with human osteoblasts (Torricelli et al., 2003; Wang et al., 2011; Zomorodian et al., 2013). Of these, Saos-2 has historically been identified as the best performing line due to its better cell proliferation and mineralization (Bilbe, Roberts, Birch, & Evans, 1996; Czekanska, Stoddart, Richards, & Hayes, 2012a), and it also exhibits osteoinductivity in vitro (Yu, Harris, Yang, Anderson, & Walsh, 2004). For Saos-2 cells, at 5 mM Mg^{2+}, enhanced proliferation capacity has historically been identified (He, Zhang, Liu, Tian, & Ma, 2016; Leidi et al., 2012). However, from 5 to

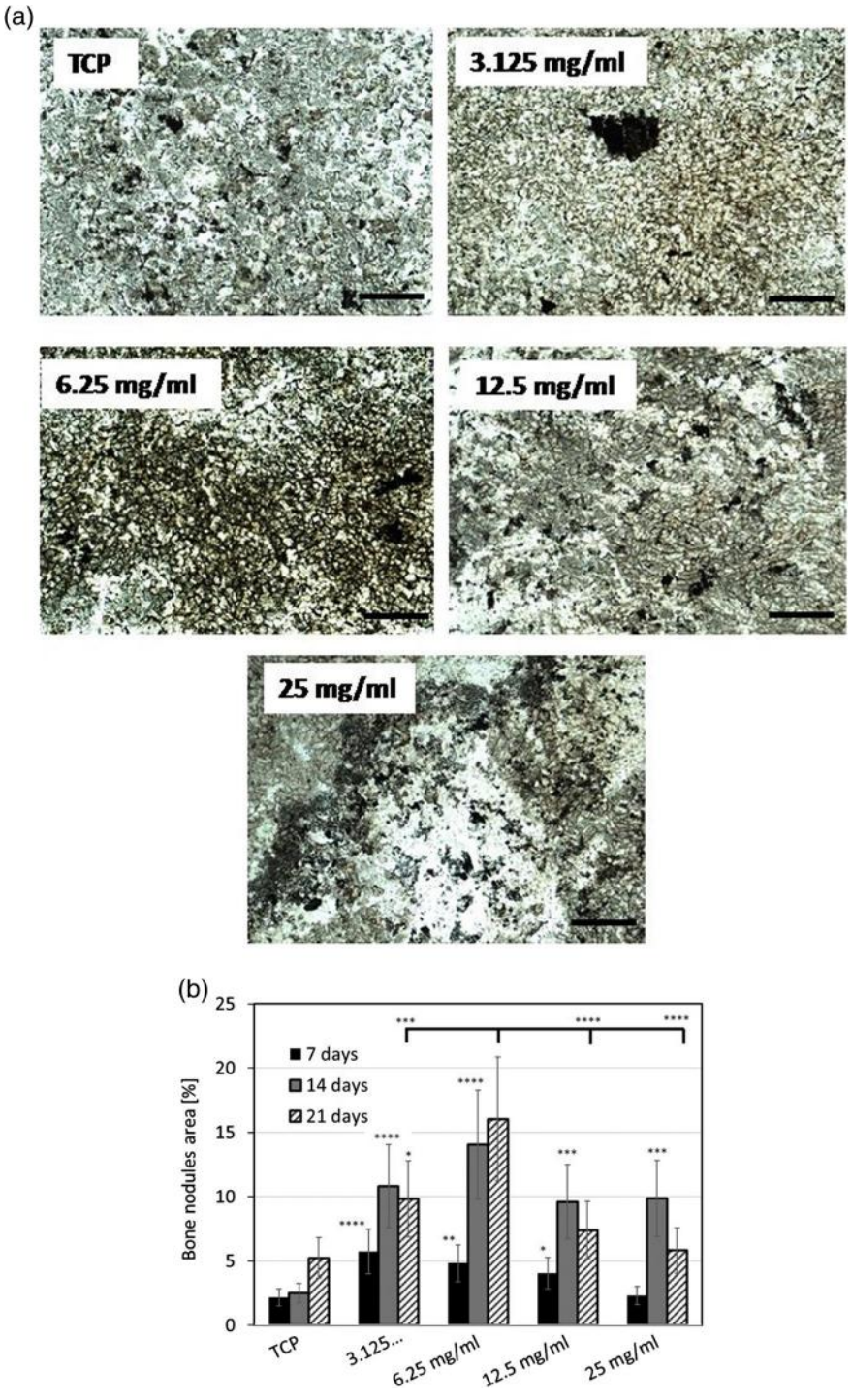

FIGURE 10 (a) Von Kossa staining using LC INSOL at various mass concentrations on Day 21 at ×10 magnifications (scale bar = 250 μm). Phosphate is indicated by black regions. (b) Quantification of Von Kossa staining area using LC INSOL at various mass concentrations on day 21 (N > 6)

25 mM, proliferation gradually reduced (as did that of the other two cell osteosarcoma cell lines, when the Mg^{2+} concentration exceeded 10 mM), although the degree of differentiation was still substantial (Sansone, Pagani, & Melato, 2013). Due to such high ion release levels, the materials synthesized need to be treated with PBS for 24 hr prior to being used with the cells in order to avoid high ion concentrations and sudden pH increases. The authors have chosen to use three osteogenic supplements with Saos-2 in this study as have many other researchers who study the effect of different stimulus on osteogenesis and matrix production in vitro (Bique, Kaivosoja, Mikkonen, & Paulasto-Kröckel, 2016). However, the authors have ensured that the concentration of dexamethasone was the same value for both the control and experimental groups. In this case, there is a clear upregulation regarding both cell differentiation and matrix production in the experimental groups that is not seen in the control groups and so this enhanced response cannot be due to spontaneous mineralization that can be seen in cell samples described in other publications (Czekanska, Stoddart, Richards, & Hayes, 2012b; Rao et al., 1996).

In our work, for Saos-2 proliferation in the presence of LC INSOL at 7 days, it was notable that LC INSOL applied at concentrations of

3.125 and 6.25 mg/mL did not significantly increase the Saos-2 cell proliferation compared with that of TCP (based on the DNA concentration data in Figure 6a) and the Mg^{2+} concentration in the culture was below 5 mM for both. However, at 14 days' cell culturing, there was a significant difference in proliferation measured between TCP and LC INSOL at 6.25 mg/mL, though not at the higher LC INSOL concentrations.

Previous literature studies have indicated that some metal ions, for example, Al^{3+}, have a detrimental effect on bone health (Lin, Wataha, & Hanks, 1997). However, usually the viability of bone cells is not adversely affected for Al^{3+} concentrations less than 1 mM (our measurements indicated that Al^{3+} concentration was consistently less than this, not shown). In addition, gene expression (i.e., that of collagen, osteocalcin and ALP) can be significantly inhibited, (Malluche, Mawad, & Monier-Faugere, 2004). Moreover, Malluche et al. indicated that even an Al^{3+} concentration of 0.2 mM is generally non-cytotoxic. Nevertheless, bone gene expression can still be down-regulated, which can cause unhealthy bone formation (Malluche et al., 2004). In addition, various other studies have shown the toxicity of Al^{3+} for organ function (e.g., it is associated with chronic renal failure) and also for bone health (Malluche, 2002; Netter et al., 1984). It has been proven that excess Al^{3+} can cause osteodystrophy and osteomalacia (Hallab et al., 2002). For this reason, potential toxicity of the Al^{3+} ions toward bone differentiation for LC INSOL cannot be ruled out in experiments reported here. Ranking metal ions in terms of their increasing effect on osteoblast cell metabolism and differentiation, the order of increasing toxicity is Na < Cr < Mg < Mo, (nontoxic or mildly toxic); Al < Ta < Co, (moderately toxic); and Ni < Fe < Cu < Mn < V, (toxic) (McComb, Bowers, & Posen, 1979).

With respect to a dual magnesium-aluminium ion effect on genetic expression, real-time PCR data indicates that the ions released from LC INSOL may accelerate the cells' differentiation. Generally, the expression of collagen Type I (COL) tracks that of ALP, that is, it increases first, and then it decreases. Osteopontin (OPN) and osteocalcin (OCN) are important gene markers for bone; osteopontin forms before osteocalcin, (Aubin, Liu, Malaval, & Gupta, 1995). Therefore, in Figure 7, at Day 14, osteocalcin showed maximal upregulated gene expression at an LC INSOL concentration of 25 mg/mL (2.65-fold increase), while at the other concentrations, normalized fold change reached only 1.9. In most cases, the gene expressions of all the selected gene markers were better regulated in samples fed with LC INSOL.

ALP is an early stage marker for cell mineralization as it tracks the concentration of alkaline phosphate enzymes, which peaks when the osteoblast matures and usually decreases again after the onset of mineralization. Figure 8 shows absolute ALP activities at 14 days in the GM alone without osteogenic inductive factors. It can be seen that magnesium had a dose-dependent effect on ALP levels during mineralization, that is, ALP activity was lower between LC INSOL solution mass concentrations of 3.125 and 12.5 mg/mL, but significantly higher at 25 mg/mL. This phenomenon is consistent with the trend shown in the data of He et al. (2016), where ALP concentration increases occurred in a Mg^{2+} concentration range of 1–3 mM. Mg^{2+} has been demonstrated as one of the essential cofactors for phosphate enzyme synthesis (Orimo, 2010), in addition to Zn^{2+} and Co^{2+}. Mg^{2+} can act similarly to Zn^{2+}; they both coenhance the enzyme activity catalytically. The mechanism for this is due to the binding sites on the phosphate enzyme subunits, between the monomers, where there are two sites for Zn^{2+} binding, one for Ca^{2+} and one for Mg^{2+} (Anderson, Bosron, Kennedy, & Vallee, 1975). In general, the more Mg^{2+} ions cells that bind, the more enzyme that is actively expressed (Dean, 2002; Tsigkou, Jones, Polak, & Stevens, 2009). Moreover, materials exposed in the OM culture medium promote cell differentiation, causing cell maturation to be slower than for the samples placed in GM alone (Ding, Pan, Xu, & Tang, 2014). For the trials using osteogenic induction factors (Figure 8) LC INSOL indicated higher ALP activity compared with that of TCP at concentrations above 6.25 mg/mL demonstrating superior performance of LC INSOL, relative to the TCP control, in promoting ALP activity.

The ability to produce nodules for cells is important for bone regeneration (Gough et al., 2004). Nevertheless, calcium phosphate formation is related to the ion concentrations leached from the materials, and the relative concentration ratio of Mg/Al is critical; when the Mg^{2+}/Al^{3+} ratio is low, only a few mineralized nodules can be formed and vice-versa. Von Kossa staining was chosen to identify phosphate deposits rather than alizarin red to stain for calcium deposits to ensure a clear reading from our image analysis data was captured. Based on the nodules area percentage calculated from the Gomori trichrome assay (Figure 9b) using ImageJ, samples at a concentration of 6.25 mg/mL exhibited the highest nodule yield at 14 and 21 days, to statistical significance, compared with the TCP control. In general, nodules consisted of crystallized CaP with a C/P ratio of 1.67 rather than the more amorphous forms of calcium phosphate (at Phase 3 of the biomineralization process as mentioned earlier (Leidi, Dellera, Mariotti, & Maier, 2011)). The extracellular matrix surrounding the cells provides the crystallization sites for the HA growth. Collagen, a fibrous protein, usually provides the template for the mineral deposition; for example, collagen is able to assist CaP deposition by immobilization of phosphoproteins (Gu et al., 2011). Therefore, the nodule formation should be consistent with the amount of collagen produced in the bone cells matrix, and this corresponds to the data found in this study (i.e., the enhanced COL gene expression in qPCR). Lastly, in addition to the effects of all the metallic ions eluted from the materials, lower pH also assists HA deposition. This is because HA is more easily dissolved in an acidic environment (Dorozhkin, 2012). This might explain why nodule formation levels in LC INSOL at 25 mg/mL are not as high as those in the 6.25 mg/mL specimen.

Mg^{2+} can be a cofactor for ALP catalytic activity. Together with β-glycerophosphate (β-Gly) in the osteogenic medium, it can be used to produce abundant phosphate groups with the help of ALP (Hayat, 2012). This is why, in the Von Kossa staining assay (Figure 8), LC INSOL at all mass concentrations indicated Mg^{2+} dose-dependent phosphate formation. Usually, phosphate ions react with Ca^{2+} to form calcium phosphate and eventually mineralize to HA. However, because of Mg^{2+} inhibition of the calcium phosphate-to-HA transition, it is believed that in this Mg^{2+} reservoir, a Mg-substituted HA might have formed. This hypothesis can be supported by the research conducted by Ding et al. (2014), where Mg^{2+} was shown to inhibit the

HA crystallization by incorporating or absorbing into the cell matrix. In general, Mg^{2+} can be easily absorbed into the mineralized matrix to restrain HA formation. The grain size of magnesium is much smaller than that of calcium; therefore, Mg-substituted HA is thought to have fewer crystalline deposits than those of Ca-HA due to a lower Mg-lattice distortion (Laurencin et al., 2011). Bone has 0.72 wt% of Mg-substituted HA (LeGeros, 1991); this proves the importance the Mg-substituted HA. However, due to limited research on Mg-substituted HA to date, its effects at higher concentrations (above 0.72 wt%) cannot be confirmed, although Mg-HA can also be beneficial for osteogenesis with enhanced BMP2 production for instance (Aubin et al., 1995; Šupová, 2015).

7 | CONCLUSIONS

This study examined the effect of a novel polymer network, based on a lactone copolymer of lactide and caprolactone (LC INSOL), on osteogenesis using the osteoblast-like cell line Saos-2. It demonstrates that LC INSOL showed superior performance to a tissue culture plastic (TCP) control with an appropriate rate-of-release of eluted magnesium ions (i.e., LC INSOL was capable of releasing a higher, more consistent concentration of Mg^{2+} ions). The effects of Mg^{2+} concentration on PN performance were studied in detail. Mg^{2+} is able to induce osteogenesis by producing ALP enzymes. Therefore, its concentration should be maintained at appropriately balanced concentrations, which depends on the overall mass concentration of LC INSOL applied. Cells were indirectly incubated with LC INSOL at 3.125 and 6.25 mg/mL mass concentrations in osteogenic culture media. Cells exposed to LC INSOL above a solution concentration of 6.25 mg/mL indicated enhanced ALP activity in GM at Day 14 compared to ALP activity in the TCP only (Figure 8). Two different hydroxyapatites (HA) (Ca- and Mg-HA) may form, depending on the PN mass concentration applied in the cell culture. The LC INSOL at 6.25 mg/mL showed the highest concentration of mineralized nodule formation in the cell matrix at all the mass concentrations investigated. By contrast, cells with the highest concentration of LC INSOL (i.e., 25 mg/mL) showed the most upregulated phosphate formation and accelerated cell differentiation. Bone-related gene expression, for example, bone morphogenetic proteins, collagen Type I, osteopontin and osteocalcin, were all upregulated in the presence of LC INSOL. All the above evidence indicates that this novel PN material, LC INSOL, has significant potential for bone tissue regeneration, and could be deployed as an acellular powder administered for osteogenesis during bone surgery after further development and verification.

ACKNOWLEDGEMENTS

This work was supported by the Engineering and Physical Sciences Research Council (EPSRC) Grant No. EP/I02249X/1.

ORCID

Edward D. McCarthy https://orcid.org/0000-0002-2038-2929

REFERENCES

Anderson, R., Bosron, W. F., Kennedy, F. S., & Vallee, B. L. (1975). Role of magnesium in *Escherichia coli* alkaline phosphatase. *Proceedings of the National Academy of Sciences of the United States of America*, *72*, 2989–2993.

Aubin, J. E., Liu, F., Malaval, L., & Gupta, A. K. (1995). Osteoblast and chondroblast differentiation. *Bone*, *17*(2,Suppl), 1,S77.

Bakhsheshian, J., Dahdaleh, N. S., Lam, S. K., Savage, J. W., & Smith, Z. A. (2015). The use of vancomycin powder in modern spine surgery: Systematic review and meta-analysis of the clinical evidence. *World Neurosurgery*, *83*, 816–823.

Bilbe, G., Roberts, E., Birch, M., & Evans, D. B. (1996). PCR phenotyping of cytokines, growth factors and their receptors and bone matrix proteins in human osteoblast-like cell lines. *Bone*, *19*(5), 437–445.

Bique, A.-M., Kaivosoja, E., Mikkonen, M., & Paulasto-Kröckel, M. (2016). Choice of osteoblast model critical for studying the effects of electromagnetic stimulation on osteogenesis in vitro. *Electromagnetic Biology and Medicine*, *35*(4), 353–364. https://doi.org/10.3109/15368378.2016.1138124

Bullough, P. P. (2010). *Orthopaedic pathology* (5th ed.). Elsevier, New York.

Chen, Q. Z., Thompson, I. D., & Boccaccini, A. R. (2006). 45S5 bioglass®-derived glass-ceramic scaffolds for bone tissue engineering. *Biomaterials*, *27*(11), 2414–2425.

Czekanska, E. M., Stoddart, M. J., Richards, R. G., & Hayes, J. S. (2012a). In search of an osteoblast cell model for in vitro research. *European Cells & Materials*, *24*, 1–17.

Czekanska, E. M., Stoddart, M. J., Richards, R. G., & Hayes, J. S. (2012b). In search of an osteoblast model for in vitro research. *European Cells & Materials*, *24*, 1–17. https://doi.org/10.22203/eCM.v024a01

Dean, R. L. (2002). Kinetic studies with alkaline phosphatase in the presence and absence of inhibitors and divalent cations. *Biochemistry and Molecular Biology Education*, *30*, 401–407.

Ding, H., Pan, H., Xu, X., & Tang, R. (2014). Toward a detailed understanding of magnesium ions on hydroxyapatite crystallization inhibition. *Crystal Growth & Design*, *14*, 763–769.

Dorozhkin, S. V. (2012). Dissolution mechanism of calcium apatites in acids: A review of literature. *World Journal of Methodology*, *2*, 1–17.

Feng, X., & McDonald, J. M. (2011). Disorders of bone remodeling. *Annual Review of Pathology: Mechanisms of Disease*, *6*, 121–145.

Gorustovich, A., Roether, J., & Boccaccini, A. R. (2010). Effect of bioactive glasses on angiogenesis: A review of in vitro and in vivo evidences. *Tissue Engineering Part B*, *16*, 199–207.

Gough, J. E., Jones, J. R., & Hench, L. L. (2004). Nodule formation and mineralisation of human primary osteoblasts cultured on a porous bioactive glass scaffold. *Biomaterials*, *25*, 2039–2046.

Gu, L. S., Kim, Y. K., Liu, Y., Takahashi, K., Arun, S., Wimmer, C. E., … Tay, F. R. (2011). Immobilization of a phosphonated analog of matrix phosphoproteins within cross-linked collagen as a templating mechanism for biomimetic mineralization. *Acta Biomaterialia*, *7*, 268–277.

Hallab, N. J., Vermes, C., Messina, C., Roebuck, K. A., Glant, T. T., & Jacobs, J. J. (2002). Concentration- and composition-dependent effects of metal ions on human MG-63 osteoblasts. *Journal of Biomedical Materials Research*, *60*, 420–433.

Hayat, M. A. (2012). Stem cells and cancer stem cells. In *Therapeutic applications in disease and injury* (Vol. 7). Springer, Netherlands.

He, L. Y., Zhang, X. M., Liu, B., Tian, Y., & Ma, W. H. (2016). Effect of magnesium ion on human osteoblast activity. *Brazilian Journal of Medical and Biological Research*, *49*, 1–6.

Hench, L. L., Splinter, R. J., Allen, W. C., & Greenlee, T. K. (1971). Bonding mechanisms at the interface of ceramic prosthetic materials. *Journal of Biomedical Materials Research*, *5*, 117–141.

Huang, W., Day, D. E., Kittiratanapiboon, K., & Rahaman, M. N. (2006). Kinetics and mechanisms of the conversion of silicate (45S5), borate, and borosilicate glasses to hydroxyapatite in dilute phosphate solutions. *Journal of Materials Science. Materials in Medicine*, *17*, 583–596.

Huang, W., Rahaman, M. N., Day, D. E., & Li, Y. (2006). Mechanisms for converting bioactive silicate, borate, and borosilicate glasses to hydroxyapatite in dilute phosphate solution. *Physics and Chemistry of Glasses - European Journal of Glass Science and Technology Part B*, *47*, 647–658.

Jones, J. R., Ehrenfried, L. M., Saravanapavan, P., & Hench, L. L. (2006). Controlling ion release from bioactive glass foam scaffolds with antibacterial properties. *Journal of Materials Science. Materials in Medicine*, *17*, 989–996.

Laurencin, D., Almora-Barrios, N., de Leeuw, N. H., Gervais, C., Bonhomme, C., Mauri, F., … Smith, M. E. (2011). Magnesium incorporation into hydroxyapatite. *Biomaterials*, *32*, 1826–1837.

LeGeros, R. Z. (1991). Calcium phosphates in oral biology and medicine. *Monographs in Oral Science*, *15*, 1–201.

Leidi, M., Dellera, F., Mariotti, M., Banfi, G., Crapanzano, C., Albisetti, W., & Maier, J. A. M. (2012). Nitric oxide mediates low magnesium inhibition of osteoblast-like cell proliferation. *The Journal of Nutritional Biochemistry*, *23*, 1224–1229.

Leidi, M., Dellera, F., Mariotti, M., & Maier, J. A. M. (2011). High magnesium inhibits human osteoblast differentiation in vitro. *Magnesium Research*, *24*, 1–6.

Lin, S. Z., Wataha, J. C., & Hanks, C. T. (1997). Effects of metal ions on osteoblast-like cell metabolism and differentiation. *Journal of Biomedical Materials Research*, *34*, 29–37.

Livak, K. J., & Schmittgen, T. D. (2001). Analysis of relative gene expression data using real-time quantitative PCR. *Methods*, *25*, 402–408.

Lv, H., Li, L., Sun, M., Zhang, Y., Chen, L., Rong, Y., & Li, Y. (2015). Mechanism of regulation of stem cell differentiation by matrix stiffness. *Stem Cell Research & Therapy*, *6*, 103–114.

Lyu, S., & Untereker, D. (2009). Degradability of polymers for implantable biomedical devices. *International Journal of Molecular Sciences*, *10*, 4033–4065.

Malluche, H. H. (2002). Aluminium and bone disease in chronic renal failure. *Nephrology, Dialysis, Transplantation*, *17*, 21–24.

Malluche, H. H., Mawad, H., & Monier-Faugere, M. C. (2004). The importance of bone health in end-stage renal disease: Out of the frying pan, into the fire. *Nephrology Dialysis Transplantation*, *19*(Suppl 1), i9–i13. https://doi.org/10.1093/ndt/gfh1002

McComb, R. B., Bowers, G. N. J., & Posen, S. (1979). *Alkaline Phosphatase.*, *116*, 633–2322.

Netter, P., Kessler, M., Burnel, D., Hutin, M. F., Delones, S., Benoit, J., & Gaucher, A. (1984). Aluminum in the joint tissues of chronic renal failure patients treated with regular hemodialysis and aluminum compounds. *The Journal of Rheumatology*, *11*, 66–70.

Orimo, H. (2010). The mechanism of mineralization and the role of alkaline phosphatase in health and disease. *Journal of Nippon Medical School*, *77*, 4–12.

Park, J. S., Chu, J. S., Tsou, A. D., Diop, R., Tang, Z., Wang, A., & Li, S. (2011). The effect of matrix stiffness on the differentiation of mesenchymal stem cells in response to TGF-β. *Biomaterials*, *32*, 3921–3930.

Rahaman, M. N., Day, D. E., Sonny Bal, B., Fu, Q., Jung, S. B., Bonewald, L. F., & Tomsia, A. P. (2011). Bioactive glass in tissue engineering. *Acta Biomaterialia*, *7*, 2355–2373.

Ramachandran, G. N., Venkatachalam, C. M., & Krimm, S. (1966). Stereochemical criteria for polypeptide and protein chain conformations: III. Helical and hydrogen-bonded polypeptide chains. *Biophysical Journal*, *6*, 849–872.

Rao, L. G., Sutherland, M. K., Reddy, G. S., Siu-Caldera, M. L., Uskokovic, M. R., & Murray, T. M. (1996). Effects of 1alpha,25-dihydroxy-16ene, 23yne-vitamin D3 on osteoblastic function in human osteosarcoma SaOS-2 cells: Differentiation-stage dependence and modulation by 17-beta estradiol. *Bone*, *19*(6), 621–627.

Sansone, V., Pagani, D., & Melato, M. (2013). The effects on bone cells of metal ions released from orthopaedic implants. A review. *Clinical Cases in Mineral and Bone Metabolism*, *10*, 34–40.

Šupová, M. (2015). Substituted hydroxyapatites for biomedical applications: A review. *Ceramics International*, *41*, 9203–9231.

Torricelli, P., Fini, M., Borsari, V., Lenger, H., Bernauer, J., Tschon, M., … Giardino, R. (2003). Biomaterials in orthopedic surgery: Effects of a nickel-reduced stainless steel on in vitro proliferation and activation of human osteoblasts. *The International Journal of Artificial Organs*, *26*, 952–957.

Tsigkou, O., Jones, J. R., Polak, J. M., & Stevens, M. M. (2009). Differentiation of fetal osteoblasts and formation of mineralized bone nodules by 45S5 bioglass® conditioned medium in the absence of osteogenic supplements. *Biomaterials*, *30*, 3542–3550.

Wang, Y. B., Xie, X. H., Li, H. F., Wang, X. L., Zhao, M. Z., Zhang, E. W., … Qin, L. (2011). Biodegradable CaMgZn bulk metallic glass for potential skeletal application. *Acta Biomaterialia*, *7*, 3196–3208.

Yamasaki, Y., Yoshida, Y., Okazaki, M., Shimazu, A., Kubo, T., Akagawa, Y., & Uchida, T. (2003). Action of FGMgCO3Ap-collagen composite in promoting bone formation. *Biomaterials*, *24*, 4913–4920.

Yamasaki, Y., Yoshida, Y., Okazaki, M., Shimazu, A., Uchida, T., Kubo, T., … Matsuura, N. (2002). Synthesis of functionally graded $MgCO_3$-apatite accelerating osteoblast adhesion. *Journal of Biomedical Materials Research*, *62*, 99–105.

Yu, Y., Harris, R. I., Yang, J.-L., Anderson, H. C., & Walsh, W. R. (2004). Differential expression of osteogenic factors associated with osteoinductivity of human osteosarcoma cell lines. *Journal of Biomedical Materials Research*, *70A*, 122–128.

Zhou, T., McCarthy, E. D., Soutis, C., & Cartmell, S. H. (2018). Lactone-layered double hydroxide networks: Towards self-assembled bioscaffolds. *Applied Clay Science*, *153*, 246–256.

Zhou, H., Wei, J., Wu, X., Shi, J., Liu, C., Jia, J., … Gan, Q. (2010). The biofunctional role of calcium in mesoporous silica xerogels on the responses of osteoblasts in vitro. *Journal of Materials Science. Materials in Medicine*, *21*, 2175–2185.

Zomorodian, A., Garcia, M. P., Moura, E., Silva, T., Fernandes, J. C. S., Fernandes, M. H., & Montemor, M. F. (2013). Corrosion resistance of a composite polymeric coating applied on biodegradable AZ31 magnesium alloy. *Acta Biomaterialia*, *9*, 8660–8670.

Zreiqat, H., Howlett, C. R., Zannettino, A., Evans, P., Schulze-Tanzil, G., Knabe, C., & Shakibaei, M. (2002). Mechanisms of magnesium-stimulated adhesion of osteoblastic cells to commonly used orthopaedic implants. *Journal of Biomedical Materials Research*, *62*, 175–184.

How to cite this article: Zhou T, McCarthy ED, Soutis C, Cartmell SH. Novel lactone-layered double hydroxide ionomer powders for bone tissue repair. *J Biomed Mater Res*. 2020; 108B:2835–2846. https://doi.org/10.1002/jbm.b.34614